Escola de Primavera de Transição e Turbulência
Blumenau 2020

ABCM Associação Brasileira de Engenharia e Ciências Mecânicas

12th Spring School on Transition and Turbulence
September 21st-25th, 2020, Blumenau, SC, Brazil

EPTT-2020-0034

NUMERICAL STUDY OF BUBBLE-INDUCED TURBULENCE MODELS IN THE DYNAMICS OF A BUBBLE COLUMN

Fabia Bocayuva Carvalho
Universidade de São Paulo
fabiabocayuva@usp.br

André Luiz Nunis da Silva
Instituto de Pesquisas Tecnológicas do Estado de São Paulo
alnunis@ipt.br

Roberto Guardani
Universidade de São Paulo
rguardani@usp.br

Abstract. *A numerical model is proposed for the complex flow of a bubble column reactor. The study was carried out in a two-dimensional dynamic simulation performed in the commercial software Fluent 2019 R2. The Euler-Euler multiphase model with interaction forces source terms was employed as well as the κ-ε turbulence model. The bubble-induced turbulence (BIT) models of Simonin and Viollet (1990) and Troshko and Hassan (2001) were investigated and compared to the zero source term standard κ-ε model. The sensitivity of both BIT models in respect to their respective coefficients (C_s, C_{ke} and C_{td}) is also studied. Different bubble sizes were tested in the Eulerian multiphase model in order to optimize the numerical results. The simulations were validated with experimental data for a bubble column presented in the literature by Sheng and Iron (1993).*

Keywords: *Numerical simulation, bubble induced turbulence, bubble columns, multiphase model, Computational fluid dynamics*

1. INTRODUCTION

Bubble columns are multiphase systems reactors with the ability of promoting mass and heat transfer between dispersed and continuous phases, as liquid, and consist of a gas phase dispersed in an homogeneous liquid, or a solid-in-liquid suspension. These systems may be found in a wide range of industries and processes, such as oxidation reactors, alkylation reactions, effluent treatments, fermentation reactors, gas cleaning systems, among others (Santos, 2005). They consist of a column equipped with a distributor, which provide injection of gas into the liquid, producing bubbly plumes and promoting the liquid motion.

Although bubble columns are considered to be of relatively simple operation and maintenance (Dionisio, 2008), they involve complex and not yet well-known flow structure. The performance of bubble columns is largely dependent on the interaction between phases present. Thus, the understanding of the flow structure is of primary importance for the adequate design of such systems.

The use of numerical simulation to predict the fluid dynamics of multiphase flows has grown and evolved with computational resources advancement. Concerning bubble columns, computational fluid dynamics (CFD) models based on fundamental conservation equations of mass and momentum have been developed to produce information related to fluid motion, as spatial distribution of phase velocities, bubble size and void fractions. Two main approaches are used to reproduce multiphase behavior in numerical simulations: Euler-Euler and Euler-Lagrange. The Euler-Euler method treats the phases as an interpenetrating continuum and models each phase separately, whereas the Euler-Lagrange is a particle tracking technique that is applied to each particle, bubble or droplet of the dispersed phase. The Lagrange technique requires significant computational demands as the effects of the dispersed phase volume fraction become large. In these cases, the advantage of the Euler-Euler method with respect to the Lagrange method is noticeable since it does not consider individual bubbles and the additional computational effort can be avoided.

The difficulty to characterize multiphase flows is mostly attributed to complex phenomena caused by the interactions between phases, which include the turbulent flow behavior revealed by energy production, transfer and dissipation (Versteeg and Malalasekera, 2007). To consider the effects of shear-induced turbulent fluctuations due to the

chaotic behavior of the flow, complex turbulence models for single phase and multiphase systems were developed, such as κ-ε and κ-ω models and Reynold Stress Model (RSM). Such models have a fundamental role in the prediction of the velocity field of bubbly plumes and multi-dimensional flows. However, in their conventional format, the turbulence models do not include the viscous shear associated with the turbulence generated in the liquid phase due to interaction with the dispersed phase. Even though the standard models can obtain adequate results, it is not physically consistent to neglect the bubble-induced turbulence in bubbly flows (Vaidheeswaran and Hikibi, 2017).

As explained by Zhang, et al., 2006, the BIT phenomenon can be accounted for by two different methods: by adding a bubble-induced turbulent viscosity term to the effective viscosity or by adding source terms to the turbulent transport equations of the multiphase turbulence models. The first approach is a simple algebraic formulation proposed by Sato and Sekoguchi (1975) based on a linear superposition of shear-induced and bubble-induced components (Vaidheeswaran and Hikibi, 2017). The second approach is a two-equation model that has been proposed in different formats (Simonin and Viollet, 1990; Troshko and Hassan, 2001; Kataoka and Serizawa, 1989; among others) and is widely used in bubble columns fluid dynamic modeling. Despite the active research on the development of suitable models for the BIT phenomenon, no consensus has been reached for a precise form of the models (Rzehak and Krepper, 2013).

This text presents results of an ongoing study, in which a numerical model was proposed to simulate the complex flow of a bubble column. The study was carried out in a two-dimensional dynamic simulation performed in the commercial software Fluent R9. The Euler-Euler multiphase model with interaction forces source terms was employed beside the κ-ε turbulence model. The bubble-induced turbulence (BIT) models of Simonin and Viollet (1990) and Troshko and Hassan (2001) were investigated and compared to the zero source term standard κ-ε model. The sensitivity of both BIT models to their respective coefficients (C_s, C_{ke} and C_{td}) was also studied. Different bubble sizes were tested in the Eulerian multiphase model in order to improve the numerical results. The simulations were validated with the physical bubble column experimental model of Sheng and Irons (1993), from literature.

2. METHODOLOGY

2.1. Mathematical model

The fluid dynamic model proposed to predict the flow field inside the bubble column must respect the conservation laws for mass and momentum, and must couple the physics of the phenomena with the variables of the governing equations. The model developed includes the governing equations for multiphase flow, turbulent properties and density of interfacial forces.

The Euler-Euler approach for multiphase flows was adopted, in which different sets of transport equations are calculated for each phase q. The phases are coupled due to the pressure field and the interaction forces, F_I, shared between them. Equations (1) and (2) refer to the continuity and momentum equations, respectively:

$$\frac{\partial(\alpha_q\rho_q)}{\partial t} + \nabla\cdot\left(\alpha_q\rho_q\vec{u}_q\right) = 0 \tag{1}$$

$$\frac{\partial(\alpha_q\rho_q\vec{u}_q)}{\partial t} + \nabla\cdot\left(\alpha_q\rho_q\vec{u}_q\vec{u}_q\right) = -\alpha_q\nabla p + \nabla\cdot\left[\alpha_q\mu_{eff,q}\left(\nabla\vec{u}_q + \nabla\vec{u}_q^T\right)\right] + \alpha_q\rho_q\vec{g} + F_I \tag{2}$$

where α_q= volume fraction of phase q, ρ_q= density of phase q, $\mu_{eff,q}$= effective viscosity of phase q, given by Eq. (3):

$$\mu_{eff,q} = \mu_{M,q} + \mu_{t,q} \tag{3}$$

where $\mu_{M,q}$= molecular viscosity and $\mu_{t,q}$= turbulent viscosity.

The lift and virtual mass forces coefficients were defined as constants with a value of 0.5 for both, while the drag force coefficient follows the Kolev model (Kolev; 2005). The drag force coefficient C_D has its value defined according to the regime in which the flow is: viscous (*vis*), distorted (*dis*), limited (*cap*).

$$\begin{aligned} &C_{D_{dis}} < C_{D_{vis}} && \rightarrow C_D = C_{D_{vis}} \\ &C_{D_{vis}} < C_{D_{dis}} < C_{D_{cap}} && \rightarrow C_D = C_{D_{dis}} \\ &C_{D_{dis}} > C_{D_{cap}} && \rightarrow C_D = C_{D_{cap}} \end{aligned} \tag{4}$$

$$C_{D_{vis}} = \frac{24}{Re}(1 + 0.1Re^{0.75}) \tag{5}$$

$$C_{D_{cap}} = \frac{8}{3}\left(1-\alpha_g\right)^2 \tag{6}$$

$$C_{D_{dis}} = \frac{2}{3}\left(\frac{d_b}{\lambda_{RT}}\right)\left\{\frac{1+17.67\left[\left(1-\alpha_g\right)^{1.5}\right]^{\frac{6}{7}}}{18.67\left(1-\alpha_g\right)^{1.5}}\right\}^2 \tag{7}$$

where Re and λ_{RT} are, respectively, the Reynolds number and the wavelength of Rayleigh-Taylor instability, given by:

$$Re = \frac{\rho_l|\vec{u}_l-\vec{u}_g|d_b}{\mu_{eff,l}} \tag{8}$$

$$\lambda_{RT} = \left(\frac{\sigma}{g\Delta\rho_{lg}}\right)^{0.5} \tag{9}$$

where d_b and σ are the bubble diameter and the surface tension between phases, respectively, which are kept constant throughout the calculations.

The turbulence properties follow the κ-ε model for each phase q by Eq. (10) and (11). The κ-ε model is based on the transport equations for the kinetic energy of turbulence κ and its dissipation ε, assuming that the flow is entirely turbulent and the effects of molecular viscosity, $\mu_{M,q}$, may be negligible. This model is coupled to the multiphase model through the volume fraction, the velocity and pressure fields, and the turbulent viscosity given by Eq. (12):

$$\frac{\partial(\alpha_q\rho_q\kappa_q)}{\partial t} + \nabla\cdot\left(\alpha_q\rho_q\kappa_q\vec{u}_q\right) = \nabla\cdot\left(\alpha_q\left(\mu_{M,q}+\frac{\mu_{t,q}}{\sigma_\kappa}\right)\nabla\kappa_q\right) + \alpha_q\left(G_\kappa-\rho_q\varepsilon_q\right) + \Pi_{\kappa,q} \tag{10}$$

$$\frac{\partial(\alpha_q\rho_q\varepsilon_q)}{\partial t} + \nabla\cdot\left(\alpha_q\rho_q\varepsilon_q\vec{u}_q\right) = \nabla\cdot\left(\alpha_q\left(\mu_{M,q}+\frac{\mu_{t,q}}{\sigma_\varepsilon}\right)\nabla\varepsilon_q\right) + \frac{\varepsilon_q}{\kappa_q}\alpha_q\left(C_{1\varepsilon}G_\kappa - C_{2\varepsilon}\rho_q\varepsilon_q\right) + \Pi_{\varepsilon,q} \tag{11}$$

$$\mu_{t,q} = \rho_q C_\mu \frac{\kappa^2}{\varepsilon} \tag{12}$$

where G_k = turbulent kinetic energy generation due to velocity gradients; $C_{1\varepsilon}, C_{2\varepsilon}, C_{3\varepsilon}$ e C_μ are constants and σ_ε e σ_κ are Prandlt turbulent numbers for ε and κ, respectively. The following values were adopted:

$$C_{1\varepsilon} = 1{,}44\,;\; C_{2\varepsilon} = 1{,}92\,;\; C_\mu = 0{,}09\,;\; \sigma_\varepsilon = 1{,}3\,;\; \sigma_\kappa = 1{,}0$$

Π_{k_q} e Π_{ε_q} are source terms used to add the phenomena associated to turbulence, as the BIT which was modeled by Simonin-Viollet (1990) and Troshko-Hassan (2001) models. Table 1 shows the equations for the source terms of both models. The source term $\Pi_{\varepsilon,q}$ in the Simonin-Viollet (1990) model is based on the time scale corresponding to the liquid phase turbulence field, whereas, in the Troshko-Hassan (2001) model, the time scale considers the contributions from drag and virtual mass forces. Also in the Troshko-Hassan (2001) model, the source term $\Pi_{\kappa,q}$ represents the work exerted by the bubble calculated through the interfacial forces and relative velocities. The standard coefficients in each model are kept as: $C_s = C_{3\varepsilon} = 1$; $C_{\kappa,e} = 0{,}75$; $C_{td} = 0{,}45$.

Table 1. Model equations of the BIT source terms in the κ-ε formulation.

Model	$\boldsymbol{\Pi_{\kappa,q}}$	$\boldsymbol{\Pi_{\varepsilon,q}}$
Simonin-Viollet (1990)	$\Pi_{\kappa,q} = C_s\alpha_q K_{gl}\vec{u}_{gl}\cdot\vec{u}_{dr}$	$\Pi_{\varepsilon,q} = C_{3\varepsilon}\frac{\varepsilon_l}{\kappa_l}\Pi_{\kappa,q}$
Troshko-Hassan (2001)	$\Pi_{\kappa,q} = C_{\kappa,e}\alpha_q K_{gl}\left\|\vec{u}_g-\vec{u}_l\right\|^2$	$\Pi_{\varepsilon,q} = C_{td}\frac{1}{\tau_g}\Pi_{\kappa,q}$; $\tau_g = \frac{2}{3}\frac{C_{VM}}{C_D}\frac{d_b}{\vec{u}_{g-\vec{u}_l}}$

2.2. Numerical details

The physical air/water system of Sheng and Irons (1993) was used to validate the numerical results obtained with the applied multiphase CFD model. The physical properties of the two phases as well as the column dimensions are shown in Tab. 2.

Table 2. Physical properties and column dimensions of the Sheng and Irons (1993) physical model.

Physical properties	**Values**
Liquid phase density (kg/m³)	998.2
Gas phase density (kg/m³)	1.225
Liquid phase viscosity (kg/m.s)	0.001
Gas phase viscosity (kg/m.s)	1.79e-5
Column dimensions	**Values**
Liquid height (m)	0.42
Column diameter (m)	0.5
Gas injector diameter (m)	0.004

The computational grid was designed in 2D geometry and in axisymmetric plane, with gas injection in the center of the column bottom at a flow rate of 50mL/s. Following a mesh sensitivity study, a mesh of 8625 elements was defined and gas mass flux at the inlet and pressure outlet were employed as boundary conditions. Both phases are treated as incompressible. No slip boundary conditions were also applied to the column wall and base for both phases. Atmospheric conditions were employed in the system and no mass or heat transfer was considered in this step of the study. The commercial CFD package Fluent 2019 R2 was used to solve the equations. Initially, the domain was considered to be filled with water and gas injection was started at time zero.

3. PRELIMINARY RESULTS

3.1. Model sensitivity to the bubble diameter

Bubble size distribution is considered a limiting factor in multiphase system modeling. It is common to assign a monodisperse distribution to polydisperse systems due to the complexity of modeling phenomena related to bubble break up and coalescence. In order to simplify the model, a monodisperse distribution according to the correlation of Morsi and Alexander (1979) was considered:

$$d_b = \left\{\left(\frac{6\sigma_l D_n}{\rho_l g}\right) + 0{,}0242\left(Q_g^2 D_n\right)^{0{,}867}\right\}^{1/6} \tag{13}$$

where D_n and Q_g are the gas injector diameter and the inlet gas flow rate, respectively.

To validate the Morsi-Alexander correlation as a monodisperse distribution, results were compared with different bubble diameter values (0.01 m and 0.001 m). Despite the background of Morsi-Alexander correlation to represent the initial bubble diameter, preliminary results showed a large deviation between experimental and numerical data. Figure 1 shows local values of the turbulence kinetic energy, the axial velocity of the liquid phase and the volume fraction of the gas at the center line along the bubble plume based on Morsi-Alexander correlation, compared with experimental data by Sheng and Irons (1993). The numerical results were collected between 1 and 2.5 seconds after start of gas injection.

Figure 1 shows that the use of larger bubble diameters, 0.0074 m and 0.01 m, underestimates the turbulence kinetic energy production and the gas volume fraction in the system. Regarding liquid phase velocity, the curves are in agreement with the experimental data by Sheng and Irons (1993). The bubble diameter acts directly on the drag force given by Eq. (14). Larger diameters correspond to a smaller interfacial transfer coefficient and, therefore, a weaker drag force, which is opposite to the upward movement of the bubble. Therefore, the decrease of the drag force results in larger axial velocities.

$$F_d = K_{gl}(\bar{u}_g - \bar{u}_l) \tag{14}$$

$$K_{gl} = \frac{3\alpha_g \alpha_l \rho_l C_d}{4 d_b}\left|\bar{u}_g - \bar{u}_l\right| \tag{15}$$

The contradiction between the results of the kinetic energy and the liquid phase velocity was explained by Sheng and Irons (1993). They argued that it can be caused by the fact that these two parameters are correlated through the effective viscosity. With low kinetic energy, the effective viscosity decreases and does not restrict the liquid phase motion and, therefore, increases its velocity.

In view of these results, a value of 0.001 m was adopted for the bubble diameter in the simulations that follow.

In all simulations, a significant discrepancy was observed between numerical and experimental results near the gas injector. It is likely that this gap occurs near the gas inlet since the flow is not yet fully developed in this region. Furthermore, it is advisable to use another calculation approach, such as Lagrangean, to capture the numerical information from this region. While in the Lagrangean approach the characteristics and development of each bubble are captured, in the Eulerian approach the focus is on the behavior of the bubble plume in general.

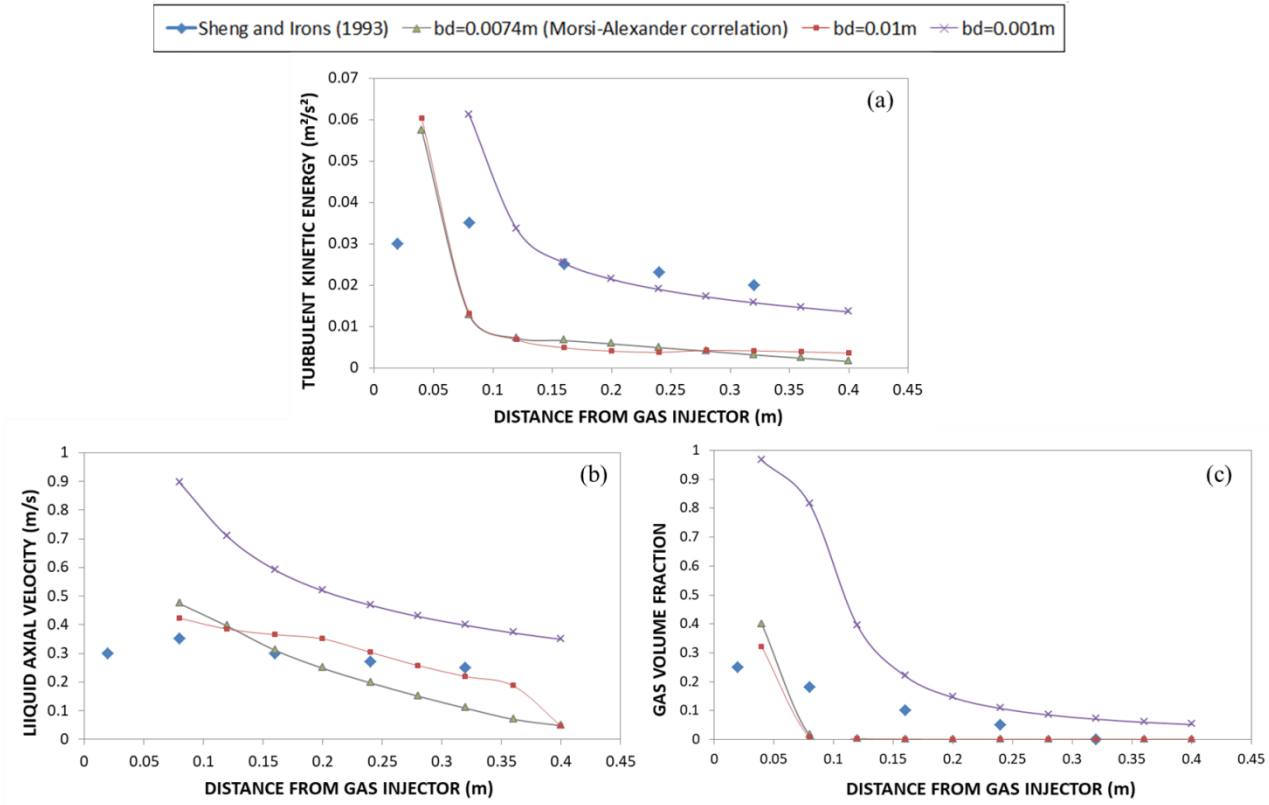

Figure 1. Comparison of numerical results for different bubble diameters as a function of the axial distance of the gas injector in terms of turbulent kinetic energy (a), liquid axial velocity (b) and gas volume fraction (c) to experimental data from Sheng and Irons (1993).

3.2. BIT models analysis

Two different models to reproduce bubble-induced turbulence in the liquid phase were tested. Figure 2 shows the local values of the turbulence kinetic energy, axial velocity of the liquid phase and volume fraction of the gas phase at the center line along the bubble plume. Data were collected between 1.5 and 6 seconds after start of gas injection.

The standard κ-ε model presents similar behavior to the Troshko-Hassan (2001) model for turbulent kinetic energy and gas volume fraction. However, Fig. 2b shows a discrepancy between the models for the axial velocity of the liquid phase. The Simonin-Viollet (1990) model overestimates the production of turbulent kinetic energy but keeps the axial velocity of the liquid close to the experimental observations. Since in this case liquid velocity is the experimental parameter obtained by measurement, and should therefore represent more reliable data, and kinetic energy is a calculated parameter, new tests were made to complement the Simonin-Viollet (1990) results. Both models have coefficients that act on the magnitude of the term in the κ-ε transport equations. Different values for these coefficients were investigated in order to improve the models in terms of their agreement with experimental data.

3.3. BIT models sensitivity to coefficients

Figures 3 and 4 show the numerical results for the correction of the coefficients of both the BIT models. The adjustment of the Simonin-Viollet (1990) model coefficient, C_s, to 0.5 resulted in better agreement of the turbulent kinetic energy to the experimental data of Sheng and Irons (1993), as well as the gas volume fraction, which shows a smaller error than that observed in Fig. 2a. In the Troshko-Hassan (2001) model, compared to Simonin-Viollet (1990) model, the correction of the coefficients did not show a significant improvement of the numerical results.

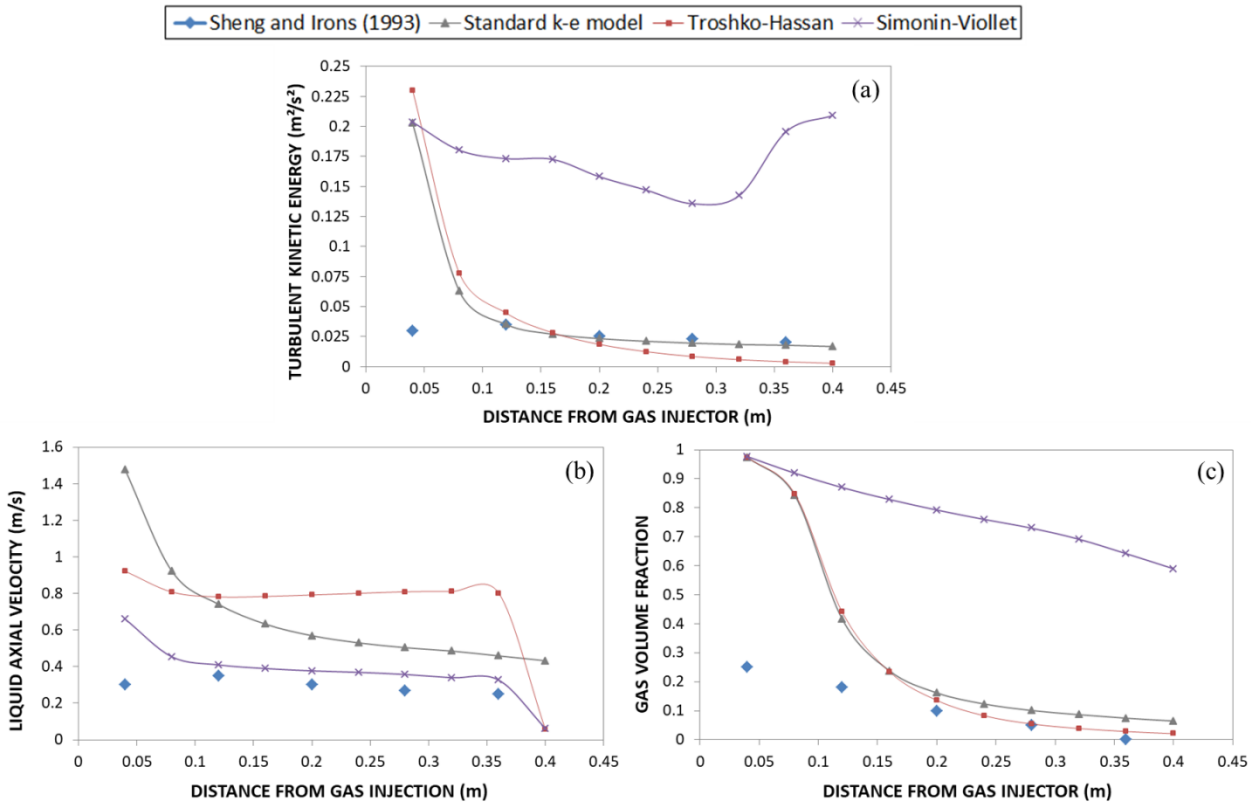

Figure 2. Comparison of numerical results for BIT models as a function of the axial distance of the gas injector in terms of turbulent kinetic energy (a), liquid axial velocity (b) and gas volume fraction (c) to experimental data from Sheng and Irons (1993).

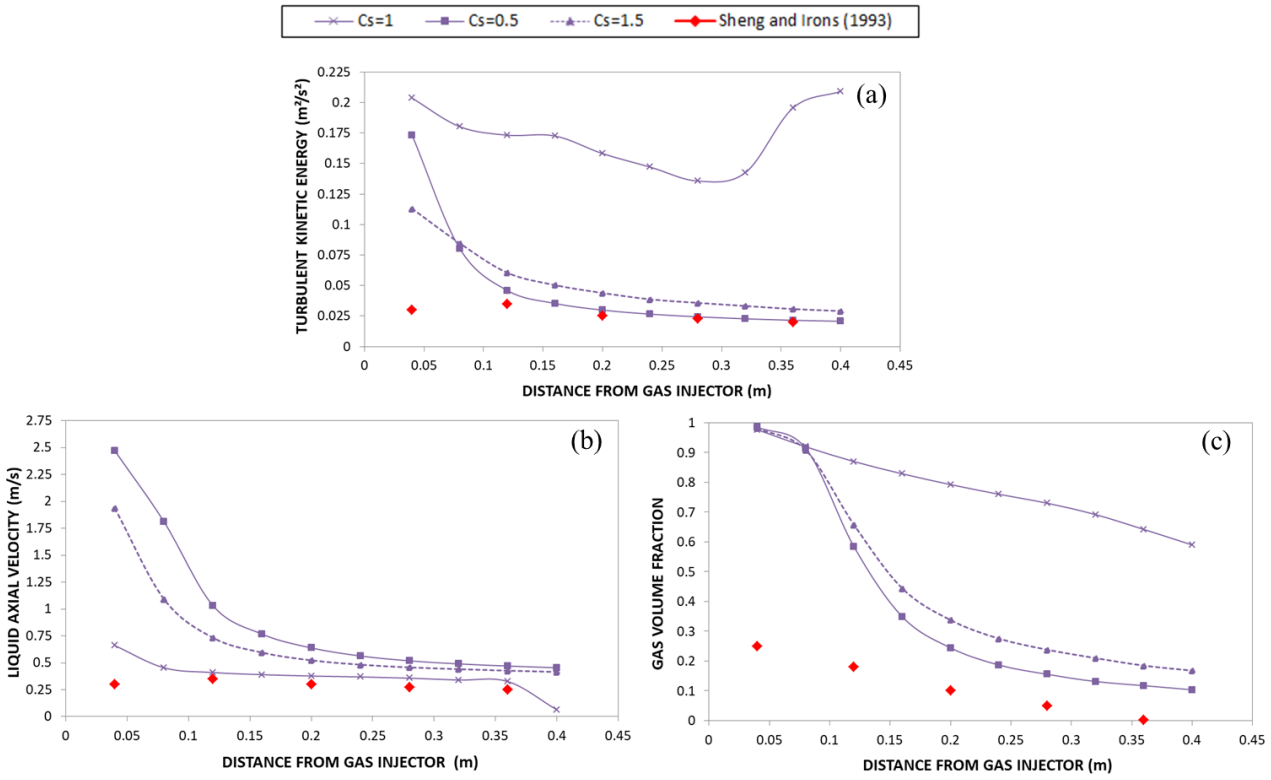

Figure 3. Numerical results for Simonin-Viollet (1990) model coefficient correction in terms of turbulent kinetic energy (a), liquid axial velocity (b) and gas volume fraction (c) compared to experimental data from Sheng and Irons (1993).

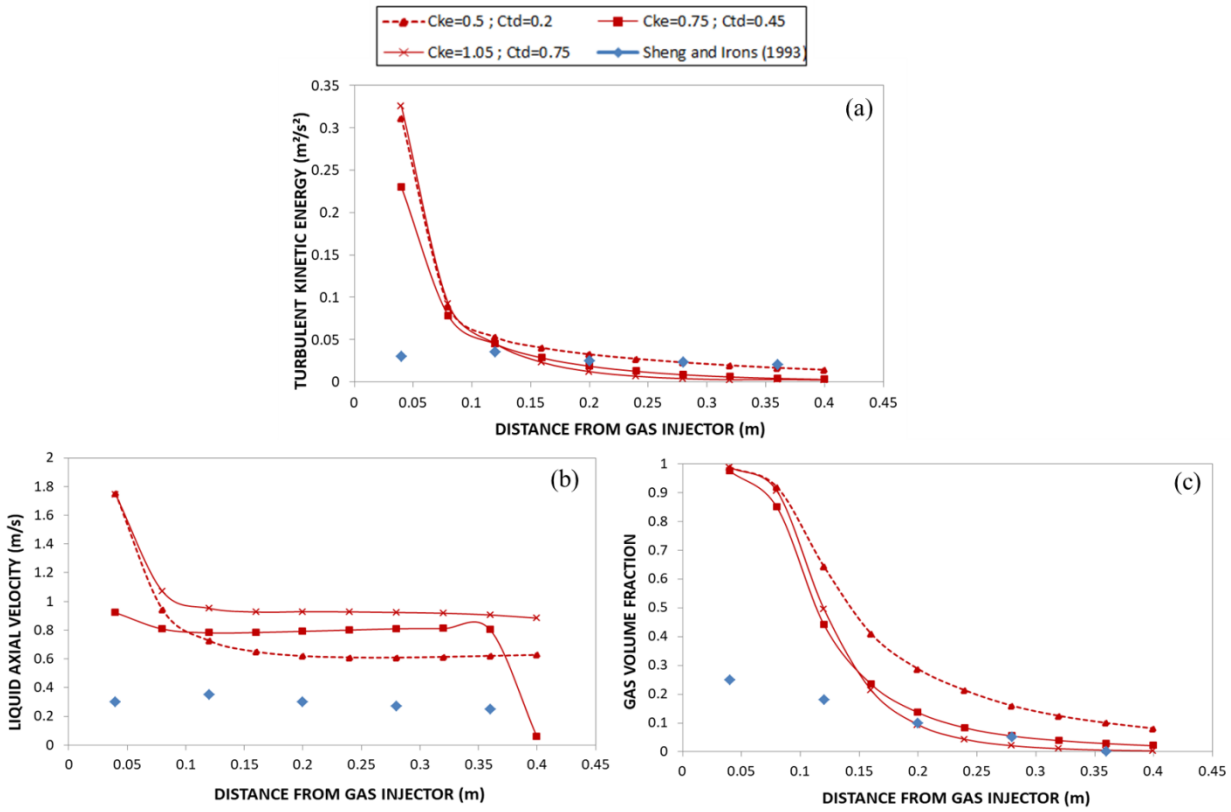

Figure 4. Numerical results for Troshko-Hassan (1990) model coefficients in terms of turbulent kinetic energy (a), liquid axial velocity (b) and gas volume fraction (c) compared to experimental data from Sheng and Irons (1993).

Figure 5 shows the liquid phase velocity vectors over the column volume. Figure 5b shows the vectors in cutting lines at different column heights. The gas inlet is located on the right bottom of Fig. 5b. The largest values of liquid phase velocity are observed near the bubble plume, despite its expansion and movement in both axial and radial directions. Figure 5a is an amplification of the area indicated in Fig. 5b, to show the liquid phase recirculation caused by the upward movement of the bubble plume. The recirculation is most evident near the surface of the liquid, where bubbles are released to the atmosphere.

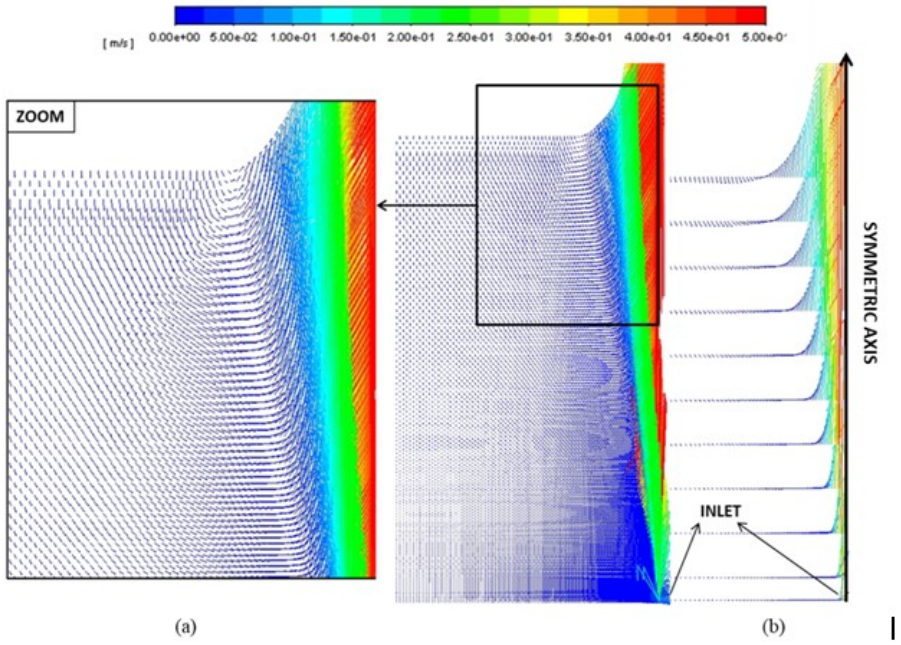

Figure 5. Magnitude vectors of the liquid phase velocities.

4. CONCLUSION

A multiphase CFD model based on bubble-induced turbulence (BIT) models was proposed and validated with experimental data collected from the literature. Interfacial forces were also considered in the applied Eulerian multiphase model. Numerical simulations were performed in the commercial CFD program Ansys Fluent 2019 R2. The sensitivity of the results to the bubble diameter and the coefficients of the BIT models were investigated. The standard κ-ε model was compared to the model including the source terms representing the turbulence associated with the inserted bubbles motion.

The flow field was accurately predicted in regions far from the gas injection for both BIT models coupled to the Eulerian multiphase model. However, neither of the BIT models showed a significant improvement in performance compared standard to the κ-ε model. The bubble diameter showed to be a parameter of large importance to the ability of the model to correctly predict the fluid dynamics, indicating that bubble interaction phenomena, such as break up and coalescence should be included. The Simonin-Viollet (1990) BIT model showed to be largely dependent on the model coefficient values.

The further development of the model shall include polydisperse bubble populations, bubble interaction phenomena (like coalescence) and a deeper understanding of the Simonin-Viollet (1990) sensitivity to the model coefficients. The discrepancy between numerical and experimental results near the gas injector should also be further investigated.

5. AKNOWLEDGEMENTS

This study is part of the Plan for Improving Research Capability in Digital Transformation: Advanced Manufacturing and Smart and Sustainable Cities, been carried at IPT (Institute for Technological Research of São Paulo State) supported by FAPESP (São Paulo State Research Support Foundation, process PDIP 17/50343). The authors are very grateful to both institutions for their support.

6. REFERENCES

DIONISIO, R. P. Simulação Tridimensional de uma Coluna de Bolhas: Diferentes Abordagens Geométricas e de Modelagem. Universidade Estadual de Campinas, 2008.

GUAN, X.; YANG, N. CFD Simulation of Pilot-Scale Bubble Columns with Internals: Influence of Interfacial Forces. Chemical Engineering Research and Design, 2017.

KATAOKA, I; SERIZAWA, A. Basic Equations of Turbulence in Gas-Liquid two phase flow. International Journal of Multiphase Flow, v 15, 1989.

KOLEV, N. I. Multiphase Flow Dynamics 2: Thermal and Mechanical Interactions. Springer, Berlin, Germany, 2nd edition. 2005.

MORSI, S. A.; ALEXANDER, A. J. An Investigation of Particle Trajectories in Two-Phase Flow Systems. J. Fluid Mech. 55(2). 193–208. September 26 1972.

RZEHAK, R.; KREPPER, E. CFD Modeling of Bubble-induced Turbulence. International Journal of Multiphase Flow, v55, 2013.

SANTOS, C. M. Simulação Tridimensional com Sistema Gás-Líquido em Colunas de Bolhas. Universidade Estadual de Campinas, 2005.

SATO, Y.; SEKOGUCHI, K. Liquid Velocity Distribution in Two-Phase Bubble Flow. International Journal of Multiphase Flow, v.2, p. 79-95, 1975.

SHENG, Y. Y.; IRONS, G. A. Measurement and Modeling of Turbulence in the Gas/Liquid Two-Phase Zone during Gas Injection. Metallurgical Transactions B, v. 24B, 1993.

SIMONIM O.; VIOLLET P. L. Modeling of Turbulent Two-Phase Jets Loaded with Discrete Particles. Phenomena in Multiphase Flows. 259–269. 1990.

TROSHKO, A. A.; HASSAN, Y. A. A Two-Equation Turbulence Model of Turbulent Bubbly Flow. International Journal of Multiphase Flow. 22(11). 1965–2000. 2001.

VAISHEESWARAN, A.; HIKIBI, T. Bubble-induced Turbulence Modeling for Vertical Bubbly Flows. International Journal for Heat and Mass Transfer, v 115, 2017.

VERSTEEG, H. K.; MALALASEKERA, W. An Introduction to Computational Fluid Dynamics: The Finite Volume Method, Second Edition, Pearson Education, 2007.

ZHANG, D.; DEEN, N. G.; KUIPERS, J. A. M. Numerical Simulations of the Dynamic Flow Behavior in a bubble column: a Study of Closures for Turbulence and Interface Forces. Chemical Engineering Science, v. 61, 2006.

7. RESPONSIBILITY NOTICE

The authors are the only responsible for the printed material included in this paper.